PROCEEDINGS OF SCIENCE

Neutral Pion Photoproduction

D.G. Middleton
Institut für Kernphysik, Universität Mainz/Mt. Allison University
E-mail: middletn@kph.uni-mainz.de

on behalf of the A2 collaboration.

Precision measurements of the differential cross sections $d\sigma/d\Omega$, the linearly polarised photon asymmetry Σ and a first measurement of the beam-target asymmetry F for the $\vec{\gamma}\vec{p} \to \pi^0 p$ reaction have been carried out at the tagged photon facility of the Mainzer Mikrotron, MAMI. The data from the Σ asymmetry measurement allow for a precise determination of the energy dependence of the real parts of the S- and all three P-wave amplitudes for the first time. Data from the second measurement are being analysed and some preliminary results are shown.

52nd International Winter Meeting on Nuclear Physics - Bormio 2014,
27-31 January 2014
Bormio, Italy

PoS(Bormio2014)015

1. Introduction

Threshold pion photo-production and the closely related process of πN scattering have long been recognised as fundamental processes, arising from the fact that the pion is the Nambu–Goldstone boson of QCD representing a clear signature of spontaneous chiral symmetry breaking [1]. A significant amount of experimental [2] and theoretical effort [3, 4] has been put into these reactions.

The production and elastic scattering of neutral pions at low energies are weak in the S-wave and strong in the P-wave [2, 3, 4, 5], as is seen in the $\gamma N \to \pi N$ reaction [6, 7]. It has also recently been shown that D-wave multipoles are important at energies close to threshold [8] and that they affect extraction of the S-wave multipole. In neutral-pion photoproduction, the S-wave threshold amplitudes are small since they vanish in the chiral limit (m_u, $m_d \to 0$); their small but nonvanishing values are consequences of explicit chiral symmetry breaking. The magnitudes of low-energy scattering and production experiments are predicted by chiral perturbation theory (ChPT), an effective field theory of QCD based on spontaneous chiral symmetry breaking [1, 3, 4, 5, 6]. Accurate measurements of low-energy $\gamma N \to \pi N$ reactions, including the spin sensitive observables that allow a unique separation of the different multipole contributions allow tests of these predictions. Any serious discrepancy between these calculations and the experimental results must be carefully examined as a challenge of our theoretical understanding of spontaneous and explicit chiral symmetry breaking in QCD [9].

Two measurements of the $\gamma p \to \pi^0 p$ reaction have been carried out to study different spin-observables. The first measurement was of the $\overrightarrow{\gamma} p \to \pi^0 p$ reaction where linearly polarised photons were incident upon an unpolarised target with the aim of obtaining the energy dependence of the photon asymmetry, Σ, for the first time and secondly the most accurate measurement to date of the differential cross section from π-threshold up to the limit of the polarisation edge of the beam, ~ 190 MeV for this measurement. The differential cross section and beam asymmetry can be expressed in terms of the S- and P-wave multipoles (E_{0^+}, P_1, P_2, P_3) with

$$\frac{d\sigma}{d\Omega}(\theta) = \frac{q}{k}\left(a_0 + a_1 \cos\theta - a_2 \cos^2\theta\right) \tag{1.1}$$

where q and k represent the c.m. momenta of the pion and photon respectively. The coefficients are given by $a_0 = |E_{o^+}|^2 + P_{23}^2$, with $P_{23}^2 = 1/2\left(|P_2|^2 + |P_3|^2\right)$, $a_1 = 2\mathrm{Re}\,(E_{o^+}P_1^*)$and $a_2 = |P_1|^2 - P_{23}^2$.

$$\Sigma(\theta) = \frac{d\sigma_\perp - d\sigma_\parallel}{d\sigma_\perp + d\sigma_\parallel} = \frac{q}{2k}\left(|P_3|^2 - |P_2|^2\right)\sin^2\theta \Big/ \frac{d\sigma}{d\Omega}(\theta) \tag{1.2}$$

where $d\sigma_\perp$ and $d\sigma_\parallel$are the differential cross sections for photon polarisation perpendicular and parallel to the reaction plane with the pion and the outgoing proton. The energy dependence of Σ, in combination with the cross-section data, allows the extraction of the real parts of all P-wave as well as S-wave multipoles as a function of photon energy. These data allow the first test of how well ChPT calculations agree with the data as a function of photon energy above threshold. This measurement has been performed before, [10], but the data were not of sufficient quality to determine all four S- and P-wave contributions individually.

The second measurement was of the F-asymmetry [11] via the $\overrightarrow{\gamma}\overrightarrow{p} \to \pi^0 p$ reaction where circularly polarised photons were incident upon a transversely polarised target. The polarised cross section $\sigma_0 F$ containing the observable F can be written as

$$\sigma_0 F(\theta) = \frac{\sigma_F^+ - \sigma_F^-}{\sigma_F^+ + \sigma_F^-} = \frac{q}{k}\sin\theta\left[f_0 + f_1\cos\theta + f_2\left((3\cos^2\theta - 1)/2\right)\right] \tag{1.3}$$

where σ_F^+ and σ_F^- are combinations of the the beam helicity, $\lambda = \pm 1$, and effective target polarisation, $s = \pm 1/2$, positive or negative with respect to the reaction plane. There are four different possible combinations though two at a time are equivalent. The coefficients f_x are sensitive to the multipole contributions. This asymmetry has never previously been measured.

2. Experimental Set-Up

The two measurements described here were carried out at the real photon facility of the A2 collaboration at the Mainzer Mikrotron (MAMI) [12]. An electron beam provided by the MAMI accelerator is directed against a radiator to produce a beam of Bremsstrahlung photons. The photon energy is determined by momentum analysing the recoil electrons using the Glasgow-Mainz Tagged Photon Spectrometer [13, 14, 15]. The photon beam is collimated and directed to the experimental area. The fraction of tagged photons passing through the collimator is measured at a reduced beam current by moving a ~100 % efficient lead glass detector into the photon beam. An ionisation chamber is used to monitor the photon flux during an experiment.

The reaction particles were detected using the Crystal Ball (CB) [16] and TAPS [17] detector set-up in the A2 hall which is shown schematically in figure 1. The CB comprises a segmented calorimeter of 672 NaI crystals covering an angular range of $21^\circ \leq \theta \leq 159^\circ$ which covers 94% of 4π steradians. Each NaI crystal has separate TDC and ADC readouts giving a time resolution of 2 ns, an angular resolution of $\Delta\theta \approx 2.5^\circ$ and energy resolution of $\Delta E \approx 3\%$. A Particle Identification Detector (PID) [18], consisting of 24 EJ204 plastic scintillators arranged in a cylinder which surrounded the target, was used to identify charged particles. The type of particle was determined using the differential energy loss measured in the PID detector, together with the energy deposited in the CB. Around the PID a set of two coaxial cylindrical MultiWire Proportional Chambers (MWPC) for charged particle tracking have been mounted of similar design to those described in [19]. Each of the MWPCs consist of three layers: inner and outer cathode strips and an anode wire layer. The wires of the anode layer are stretched parallel to the cylinder axis while the cathode strips are wound helically at an angle of $\pm 45^\circ$ with respect to the anode wires. The MWPC has a resolution of $\Delta\theta \approx 2^\circ$ and $\Delta\phi \approx 3^\circ$. Downstream of the CB the TAPS detector array has been located and it covered an angular range of $2 \leq \theta \leq 20^\circ$. TAPS consists of 366 hexagonal BaF_2 crystals and two inner rings of 72 $PbWO_4$ crystals. Each BaF_2 crystal and set of 4 $PbWO_4$ crystals has its own 5 mm thick veto paddle for charged particle identification. TAPS has an angular resolution of $\Delta\theta \approx 0.7^\circ$ and energy resolution of $\Delta E \approx 3\%$.

2.1 $d\sigma/d\Omega$ and Σ

For this measurement an electron beam of 855 MeV was directed against a 100 μm diamond radiator to produce a beam of linearly polarised photons [20]. The diamond was aligned so that the coherent edge of the polarisation peak was at an incident photon energy of $E_\gamma \sim 190$ MeV which delivered a beam polarisation of $40 - 70\%$ from π-threshold to the polarisation peak. Measurements with the lead glass detector and diamond radiator allowed for absolute measurements of the

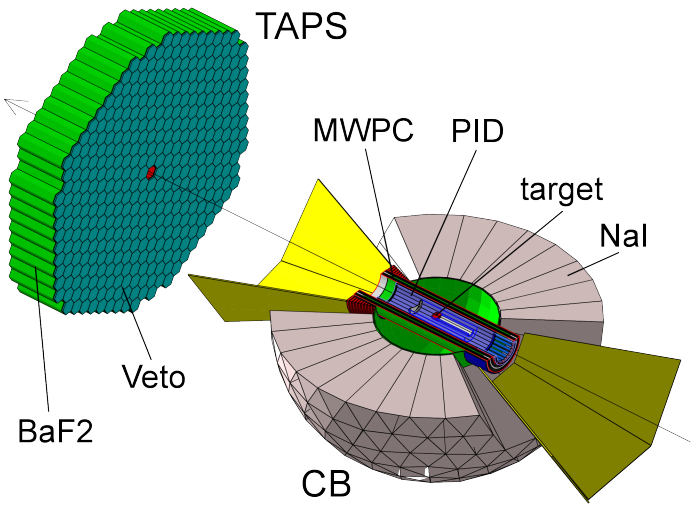

Figure 1: A schematic diagram of the Crystal Ball-TAPS set-up in A2 with the beam travelling from bottom-right to top-left . The PID and MWPCs can be seen in the centre of the CB. See the main text for more details.

beam polarisation at regular intervals. At this incident electron energy photon energy resolutions of 1.2 -2.0 MeV were achieved.

The photon beam was incident upon a 10-cm-long liquid hydrogen (LH_2) target located in the centre of the CB. Empty-target measurements were carried out to correct for events originating in the target cell material.

2.2 F asymmetry

For this measurement a beam of circularly polarised Bremsstrahlung photons was produced by directing a beam of longitudinally polarised electrons of energy 450 MeV against a 10 μm copper radiator. With this incident electron energy photon energy resolutions of 0.5 - 1.5 MeV were achieved. The electron beam polarisation was measured periodically using a Mott polarimeter located in the electron beam line [21].

For the majority of the data taking a butanol 'frozen-spin target' (FST) [22] was used to provide the polarised hydrogen necessary for the measurement. This was operated at 0.025 K and consisted of beads of polarised butanol in a liquid ^{3}He/^{4}He bath. The FST target cell was 2 cm long and had a target thickness of $N_T \approx 9.1 \times 10^{22}$ cm^{-2} with an average proton polarisation of $P_p = 70\%$. Typically the target was repolarised every 5-6 days and the direction of the polarisation flipped during repolarisation to reduce systematic effects.

To account for reactions in the ^{12}C and ^{16}O in the FST, data were taken with a 'carbon-foam' target in place within the FST cryostat. The length was the same as the FST and the density chosen so that the number of nuclei would match the total number of non-hydrogen nuclei in the FST; see [23] for more details.

The trigger for the measurement was a simple CB energy sum which included all crystals in the CB; the threshold was set at $E_{sum} \geq 100$ MeV.

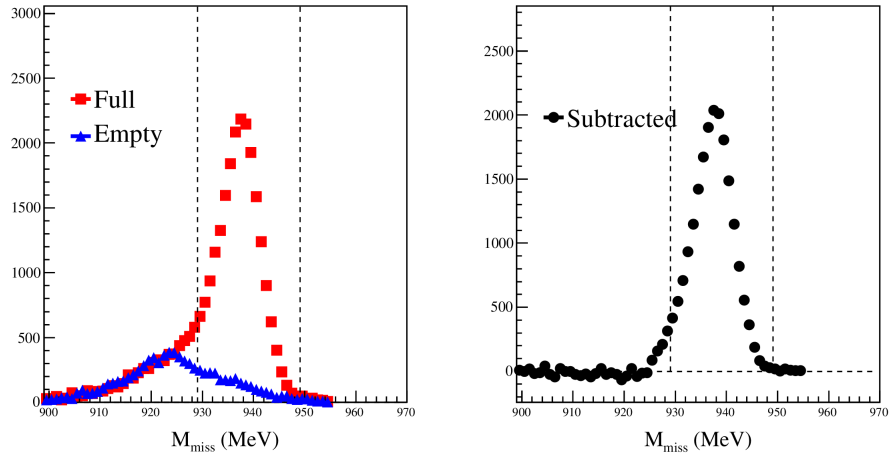

Figure 2: Example of subtraction of events where the π^0 was produced in the target cell material for $E_\gamma = 163 \pm 1.2$ MeV.

3. Measurement of $d\sigma/d\Omega$ and the Σ asymmetry

The results of this measurement have been previously published in [24] and full details regarding the analysis of the data can be found there. Neutral pions produced were identified in the detector system from their decay into two photons via the reaction $\gamma p \to \pi^o p \to \gamma\gamma p$. To determine events of interest a kinematic fitting technique described in [25] was used where events with a probability of $\geq 2\%$ were accepted. There were two main sources of background events identified in the analysis, the first were events where the reconstructed π^0 was detected in accidental coincidence with an electron in the tagger; such events were removed using a prompt coincidence cut on the electron π^0 coincidence time spectrum and subtracting an accidental sample from this. The second source were from events where the π^0 was produced in material in the target cell walls. In order to reject these background events, data collected with an empty-target cell were analysed and subtracted after proper normalisation from the full target data. An example of this can be seen in figure 2 for an incident photon energy of $E_\gamma = 163 \pm 1.2$ MeV. The geometrical acceptance of the detector system was determined by Monte Carlo simulation of the $\gamma p \to \pi^0 p$ reaction using an isotropic angular distribution. All events were then propagated through a GEANT3.21 simulation of the experimental set-up, folded with resolutions of the detectors and conditions of the trigger.

After the selection of good events and correction for detection efficiencies and luminosity the differential cross sections and Σ were determined for a range of incident photon energy and angular bins, see [24]. A PWA of these quantities was performed to extract the multipole amplitudes and compare them to theoretical calculations. The coefficients of these multipoles are shown as a function of E_γ in figure 3. The measurement of $d\sigma/d\Omega$ and Σ allow all four of the above S- and P-wave multipoles to be extracted independently and due to the high quality of the data this is the first measurement to have been able to do this. A more complete description of the results and theoretical comparison can be found in [24].

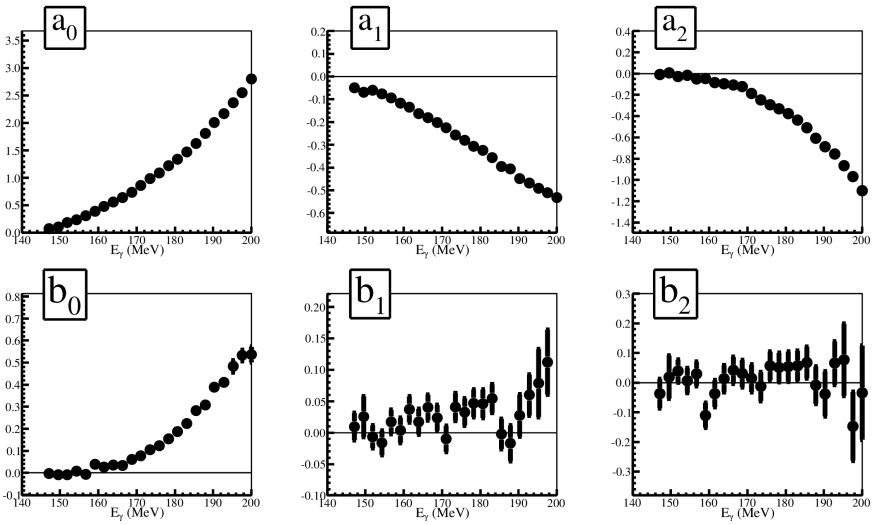

Figure 3: The coefficients of the multipole extraction from equations 1 and 2 and shown as a function of E_γ.

4. Measurement of the F asymmetry

The measurement of the $\vec{\gamma}\vec{p} \to \pi^0 p$ was carried out for the first time and the analysis of the data is still ongoing [26]. As in section 3 events of interest were determined using the two photon decay of the π^0 using the $\gamma p \to \pi^o p \to \gamma\gamma p$ reaction. After reconstruction of the π^0 4-vector the missing mass of the reaction was determined using that and information on the incident photon from the tagger. For events originating from the $\gamma p \to \pi^o p$ reaction this should be equal to the missing mass of the proton. With the Butanol target events produced from the quasi-free or coherent π^0 production reaction on the ^{12}C and ^{16}O nuclei can also occur. Such events cause a broadening of the missing mass peak due to the the Fermi motion. To reduce the effect of these energy dependent selections were applied to isolate the quasi-free and coherent processes from the free proton contributions [26]. For events where the reconstructed π^0 was detected in accidental coincidence with an electron in the tagger a subtraction was made as described in section 3. An example missing mass spectrum for $E_\gamma = 190 \pm 0.8$ MeV can be seen in figure 4 after the accidental correction has been applied.

The polarised cross section $\sigma_0 F$ was determined for the two beam helicity states after applying corrections for energy and angular event detection efficiency (determined using a Geant4 simulation of the CB-TAPS set-up), target polarisation, beam polarisation and normalising the data with the determined luminosity. Corrections for events originating from non-hydrogen nuclei were determined using data taken with the carbon-foam target. After this the F asymmetry could be determined and an example for $E_\gamma = 180 \pm 0.8$ MeV is shown in figure 5. The curves shown are different theoretical predictions for the asymmetry: red [27], blue [28], green [29] and black[30, 31]. As can be seen all show a reasonable agreement with the data.

Figure 6 shows some preliminary results for the expansion defined in equation 1.3 compared to the same theoretical models as figure 5. The shape of the measured data are reasonably well described by the different calculations though the magnitude of the asymmetry is not always well

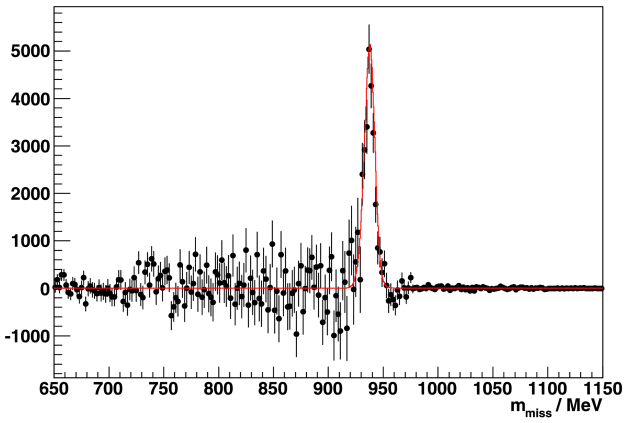

Figure 4: Missing mass spectrum for $E_\gamma = 190 \pm 0.8$ MeV for the $\gamma p \to \pi^o p$ from the Butanol target.

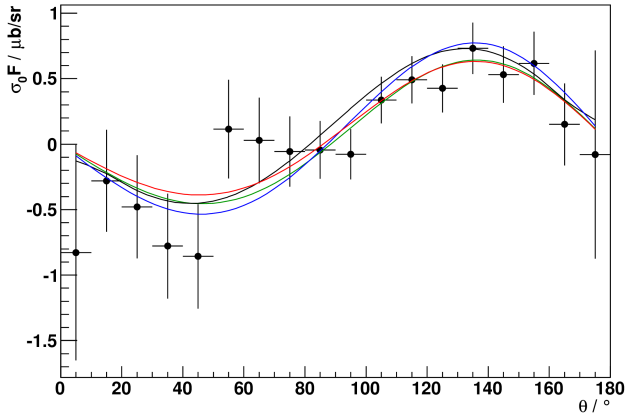

Figure 5: Preliminary results for the F asymmetry determined for $E_\gamma = 180 \pm 0.8$ MeV compared to different theoretical predictions. See the text for details of the curves.

described. With the f_2 coefficient the calculations predict a change in sign of the asymmetry at $E_\gamma \sim 340$ MeV which is not not seen with the data. The analysis of the experimental data must be finalised before any definite comparisons can be made with the models.

5. Conclusions

Two measurements of the $\gamma p \to \pi^0 p$ reaction have been made from threshold energies up to study different spin-observables of the reaction. The first measurement where linearly polarised photons were incident upon an unpolarised target has studied the differential cross section with high precision and has the first results for the energy dependence of the beam asymmetry, Σ. Using these data it has been possible to separate the S- and three P-wave multipoles contributions for

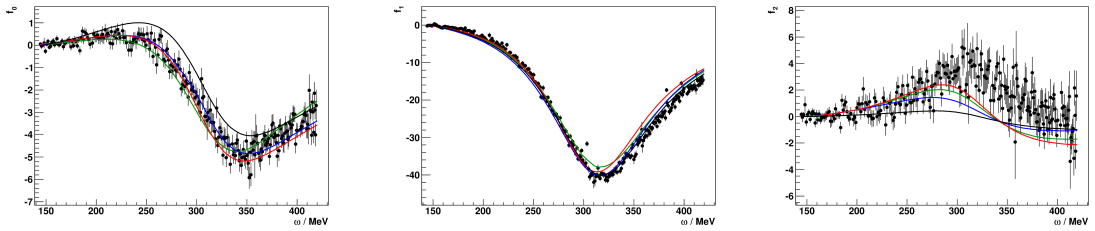

(a) f_0 (b) f_1 (c) f_2

Figure 6: Expansion of the $\sigma_0 F$ cross section as a function of E_γ compared to different theoretical predictions. The coefficients are those in equation 3, see the text for details of the curves.

the first time. The second measurement where circularly polarised photons were incident upon a transversely polarised target studied the F asymmetry. Analysis of these data is still ongoing.

References

[1] J.F. Donoghue, E. Golowich, and B.R. Holstein. *Dynamics of the Standard Model*. Cambridge University Press, Cambridge, England, 1994.

[2] A.M. Bernstein, M.W. Ahmed, S. Stave, Y.K. Wu, and H. Weller. *Ann. Rev. Nucl. Part. Sci.*, 59:115, 2009.

[3] V. Bernard and U.G. Meißner. *Ann. Rev. Nucl. Part. Sci.*, 57:33, 2007.

[4] V. Bernard. *Prog. Part. Nucl. Phys.*, 60:82, 2008.

[5] S. Scherer and M.R. Schindler. *Lect. Notes Phys.*, 830:1, 2012.

[6] S. Scherer and D. Drechsel. *J. Phys. G*, 18:449, 1992.

[7] S. Weinberg. *I. I. Rabi Festschrift*, volume 38, page 185. New York Academy of Sciences, New York, 1977.

[8] C. Fermández Ramirez, A.M. Bernstein, and T.W. Donnelly. *Phys. Lett. B*, 679:41, 2009.

[9] A.M. Bernstein. *Chiral Dynamics: Theory and Experiment*, page 3. World Scientific, New Jersey, 2007.

[10] A. Schmidt et al. *Phys. Rev. Lett.*, 87:232501, 2001.

[11] I.S. Barker, A. Donnachie, and J.K. Storrow. *Nucl. Phys. B*, 95:347, 1975.

[12] K.H. Kaiser et al. *Nucl. Instr. and Meth. in Phys. Res. A*, 593:159, 2008.

[13] J.C. McGeorge et al. *Eur. Phys. J. A*, 37:129, 2008.

[14] I. Anthony et al. *Nucl. Inst. and Meth. A*, 301:230, 1991.

[15] S.J. Hall et al. *Nucl. Inst. and Meth. A*, 368:698, 1996.

[16] A. Starostin et al. *Phys. Rev. C*, 64:055205, 2001.

[17] R. Novotny. The BaF-2 photon spectrometer TAPS. *IEEE Trans. Nucl. Sci.*, 38:379, 1991.

[18] D. Watts. In *Calorimetry in Particle Physics, Proceedings of the 11th International Conference, Perugia, Italy 2004*. Edited by C. Cecchi, P. Cenci, P. Lubrano, and M. Pepe (World Scientific, Singapore, 2005, p. 560), 2005.

[19] G. Audit et al. *Nucl. Inst. and Meth. A*, 301:473, 1991.

[20] D. Lohmann et al. *Nucl. Inst. and Meth. A*, 343:494, 1994.

[21] K-H. Steffens, H.G. Andresen, J. Blume-Werry, and F. Klein. *Nucl. Instr. and Meth. in Phys. Res. A*, 325:378, 1993.

[22] A. Thomas. *Eur. Phys. J. Special Topics*, 198:171, 2011.

[23] P.P. Martel. *Measuring proton spin polarizabilities with polarized compton scattering*. PhD thesis, University of Massachusetts Amherst, 2013.

[24] D. Hornidge et al. *Phys. Rev. Lett.*, 111:062004, 2013.

[25] S. Prakhov et al. *Phys. Rev. C*, 79:035204, 2009.

[26] S. Schuman. Private Communication.

[27] D. Drechsel et al. *Eur. Phys. J. A*, 34:69, 2007.

[28] R. Workma et al. *Phys. Rev. C*, 85:025201, 2012.

[29] S.S. Kamalov et al. *Phys. Rev. C*, 64:032201, 2001.

[30] A.V. Anisovich et al. *Eur. Phys. J. A*, 47:153, 2011.

[31] A.V. Anisovich et al. *Eur. Phys. J. A*, 48:15, 2012.

[32]